Journal of Magnetic Resonance **140,** 340–346 (1999)
Article ID jmre.1999.1825, available online at http://www.idealibrary.com on IDEAL®

Two- and Three-Dimensional $^{1}H/^{13}C$ PISEMA Experiments and Their Application to Backbone and Side Chain Sites of Amino Acids and Peptides

Zhengtian T. Gu and Stanley J. Opella[1]

Department of Chemistry, University of Pennsylvania, Philadelphia, Pennsylvania 19104

Received October 16, 1998; revised May 27, 1999

Two-dimensional $^{1}H/^{13}C$ polarization inversion spin exchange at the magic angle experiments were applied to single crystal samples of amino acids to demonstrate their potential utility on oriented samples of peptides and proteins. High resolution is achieved and structural information obtained on backbone and side chain sites from these spectra. A triple-resonance experiment that correlates the $^{1}H–^{13}C_{\alpha}$ dipolar coupling frequency with the chemical shift frequencies of the α-carbon, as well as the directly bonded amide ^{15}N site, is also demonstrated. In this experiment the large $^{1}H–^{13}C_{\alpha}$ heteronuclear dipolar interaction provides an independent frequency dimension that significantly improves the resolution among overlapping ^{13}C resonances of oriented polypeptides, while simultaneously providing measurements of the $^{13}C_{\alpha}$ chemical shift, $^{1}H–^{13}C$ dipolar coupling, and ^{15}N chemical shift frequencies and angular restraints for backbone structure determination.

Key Words: **PISEMA; solid-state NMR spectroscopy; dipolar coupling; protein structure determination; amino acid; single crystal; triple-resonance; peptide.**

INTRODUCTION

Multidimensional solid-state NMR experiments incorporating spin-exchange at the magic angle (SEMA) (*1*) are proving to be extremely valuable in applications to ^{15}N-labeled peptides and proteins (*2–5*). The very high resolution of the heteronuclear dipolar coupling frequency dimension makes it feasible to resolve many individual resonances in spectra obtained from ^{15}N-labeled proteins in supramolecular structures, including membrane bilayers (*4*, *5*) and virus particles (*3*). Since the proteins in these structures are immobile on the relevant NMR timescales, the well-resolved spectra demonstrate that there is no fundamental size limitation to the molecules that can be studied with NMR spectroscopy due to line-broadening that is a consequence of slow molecular reorientation. Further, these experiments enable the measurement of multiple orientationally dependent frequencies that provide input for protein structure determination by solid-state NMR spectroscopy (*6*).

Now that it is possible to obtain completely resolved solid-state NMR spectra of uniformly ^{15}N-labeled proteins (*4*), the development of methods for making backbone resonance assignments and of examining side chain sites has a high priority. We have recently demonstrated that it is possible to assign amide backbone resonances utilizing ^{13}C chemical shift/^{15}N chemical shift correlation experiments and to measure spectral parameters associated with both ^{13}C- and ^{15}N-labeled sites for structure determination in peptides (*7*) and proteins (*8*). Proteins uniformly labeled with ^{13}C by expression in bacteria have all side chain sites labeled, in addition to backbone sites. The resolution of ^{13}C side chain resonances provides an opportunity for determining the full three-dimensional structures of proteins. Side chain ^{13}C sites present a wide variety of chemical shift tensors and C–H bonding arrangements, in contrast to the uniformity of ^{13}C and ^{15}N backbone sites. Surveys of the chemical shift tensors of various organic and inorganic compounds, including amino acids, have been published (*9–11*). Significantly, the frequencies associated with $^{1}H–^{13}C$ heteronuclear dipolar couplings are more than twice as large as those for ^{1}H-^{15}N couplings, thus, they offer even better possibilities for spectral resolution in the heteronuclear dipolar coupling frequency dimension of multidimensional solid-state NMR spectra.

The spectral manifestations of heteronuclear dipolar couplings reflect the gyromagnetic ratios of the nuclei, the number of bonded nuclei, the bond lengths, and the angles between the bonds and the direction of the applied magnetic field in oriented samples. The seminal two-dimensional separated local field experiment has been used to characterize the dipolar couplings of CH, CH_2, and CH_3 groups in single-crystal samples (*12*). Polarization inversion schemes have also been shown to distinguish among these same chemical groups (*13*). Utilizing three-dimensional correlation spectroscopy on a polycrystalline sample of a peptide, we have characterized the ^{1}H chemical shift, $^{1}H–^{13}C$ dipolar coupling, and ^{13}C chemical shift tensors of an α carbon in a peptide (*14*). It has been demon-

[1] To whom correspondence should be addressed at Department of Chemistry, University of Pennsylvania, 231 South 34th Street, Philadelphia, PA 19104. E-mail: opella@sas.upenn.edu. Fax: (215)-573-2123.

1090-7807/99 $30.00

strated theoretically that a single unique structure can be obtained when the frequencies from ^{1}H–^{15}N, ^{15}N–^{13}C, and $^{13}C_{\alpha}$–^{1}H dipolar couplings are considered together, while it is not sufficient to define the peptide plane based on only the orientation of N–H and N–C bonds (*15*). The combination of ^{15}N chemical shift, ^{13}C chemical shift, ^{1}H–^{15}N dipolar coupling, and ^{1}H–^{13}C dipolar coupling frequencies improves the accuracy of structure determination compared to what is possible with the frequencies associated with only the ^{15}N amide site. It has also been shown that the $^{1}H_{\alpha}$–$^{13}C_{\alpha}$ dipolar coupling can be measured in solution NMR spectra, and the backbone dihedral angle ψ can be determined based on the cross-relaxation between the $^{1}H_{\alpha}$–$^{13}C_{\alpha}$ dipolar coupling and the ^{13}C chemical shift anisotropy (*16–18*).

In this Article we describe the application of the two-dimensional polarization inversion spin exchange at the magic angle (PISEMA) experiment (*1*) to single-crystal samples of aliphatic and aromatic amino acids and demonstrate that high resolution can be achieved and structural parameters measured for both backbone and side chain ^{13}C sites. We also demonstrate a triple-resonance experiment that correlates the ^{1}H–$^{13}C_{\alpha}$ dipolar coupling frequency with the $^{13}C_{\alpha}$ and ^{15}N amide chemical shift frequencies. The large ^{1}H–$^{13}C_{\alpha}$ heteronuclear dipolar coupling provides an independent frequency dimension that helps resolve among overlapping ^{13}C resonances, enabling the measurement of the $^{13}C_{\alpha}$ chemical shift, ^{1}H–^{13}C dipolar coupling, and ^{15}N chemical shift frequencies for backbone structure determination.

The two-dimensional experiment is demonstrated with spectra of single crystal samples of natural abundance *N*-acetyl valine (NAV) and tyrosine hydrochloride, which serve as examples of a variety of side chain carbon sites. The three-dimensional experiment is applied to a single-crystal sample of 2,4-^{13}C, 3-^{15}N-labeled *N*-acetylglycine (NAG). The crystal structures of *N*-acetylvaline (*19*), tyrosine hydrochloride (*20*), and *N*-acetylglycine (*21*) have been determined, and they have all been shown to have two magnetically inequivalent molecules in their asymmetric unit. Their two-dimensional $^{1}H/^{13}C$ PISEMA spectra demonstrate that it is possible to measure heteronuclear dipolar couplings associated with all carbon functional groups found in proteins, including those without directly bonded hydrogens. ^{1}H–$^{13}C_{\alpha}$ spectral slices provide angular information that can be used to determine the orientations of side chains. The three-dimensional ^{1}H–$^{13}C_{\alpha}$ dipolar coupling/$^{13}C_{\alpha}$ chemical shift/^{15}N chemical shift spectrum is displayed as a cube that can be analyzed as ^{15}N chemical shift resolved two-dimensional ^{1}H–$^{13}C_{\alpha}$ coupling/^{13}C shift planes for individual amide sites.

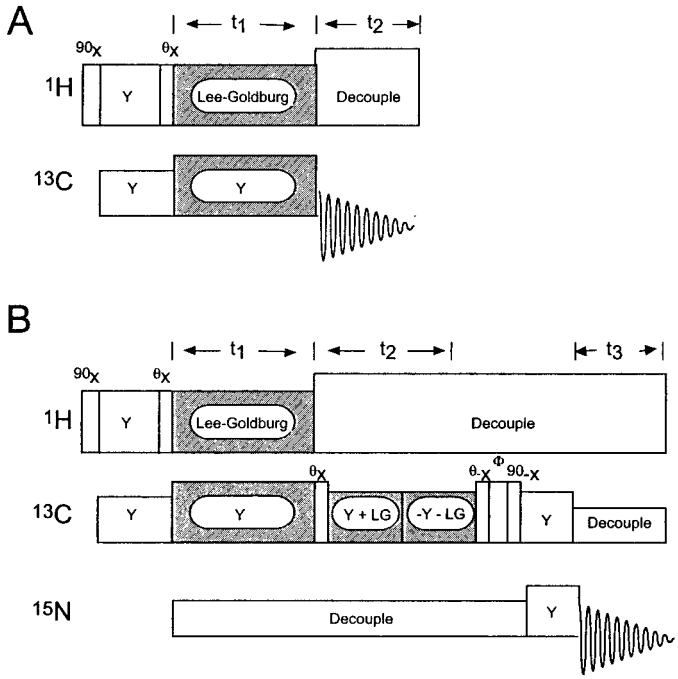

FIG. 1. A. Pulse sequence that generates two-dimensional ^{1}H–^{13}C dipolar coupling/^{13}C chemical shift spectra. B. Pulse sequence that generates three-dimensional, triple-resonance ^{1}H–^{13}C dipolar coupling/^{13}C chemical shift/^{15}N chemical shift spectra. Each t_2 increment corresponds to an integral number of cycles defined by the flip–flop Lee–Goldburg irradiation.

RESULTS AND DISCUSSION

The two- and three-dimensional pulse sequences diagrammed in Fig. 1 incorporate spin-exchange at the magic angle (*1*) in one of the incremented periods, enabling the evolution of the carbon magnetization according to the ^{1}H–^{13}C dipolar coupling interaction with minimal interference from homonuclear ^{1}H dipolar couplings. The two-dimensional ^{13}C experiment diagrammed in Fig. 1A is essentially the same as that described previously for ^{15}N (*1*), since it can be performed with either continuous (*22*) or flip–flop Lee–Goldburg (*23, 24*) irradiation during the t_1 interval. This experiment is intended for natural abundance or specifically labeled samples, since it does not include homonuclear ^{13}C decoupling (*7, 25*), which is required for high-resolution spectroscopy with uniformly ^{13}C-labeled samples. The experiment starts with the transfer of ^{1}H magnetization to ^{13}C by conventional spin-lock cross-polarization (*26*). The magnetization then evolves under the ^{1}H–^{13}C dipolar interaction during the t_1 interval. ^{13}C signals are detected during the t_2 interval in the presence of ^{1}H irradiation for heteronuclear decoupling. The large range of ^{1}H–^{13}C dipolar coupling frequencies (0–25 kHz) means that very short cycle times are required during t_1 to avoid alaising. As a result, in some situations it is simpler to utilize continuous off-resonance Lee–Goldburg irradiation during t_1 than to raise the RF power levels to give the 90° pulse lengths needed for short cycle times. Although this results in somewhat broader linewidths in the heteronuclear dipolar coupling frequency dimension than observed with flip–flop Lee–Goldburg procedures (800 vs 400 Hz), it allows for arbitrarily short increments in t_1. The ^{1}H–^{13}C

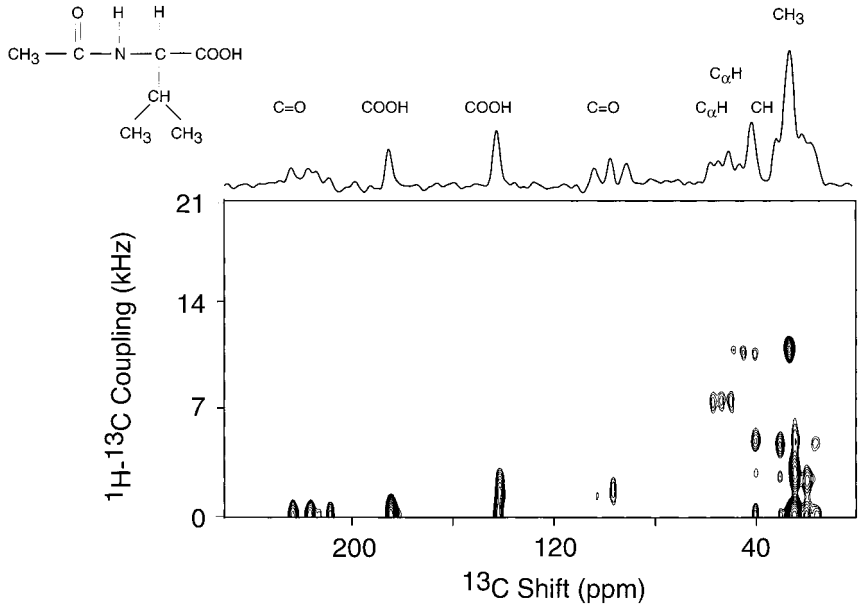

FIG. 2. Experimental two-dimensional ^{1}H–^{13}C dipolar coupling/^{13}C chemical shift spectrum of a single-crystal sample of natural abundance NAV at an arbitrary orientation with respect to the applied magnetic field. The assignments of chemical group types for each individual peak are indicated on the one-dimensional ^{13}C NMR spectrum at the top of the figure.

heteronuclear dipolar coupling frequencies are scaled by 0.82 in either case.

The pulse sequence for the three-dimensional ^{1}H–^{13}C dipolar coupling/^{13}C chemical shift/^{15}N chemical shift experiment shown in Fig. 1B is suitable for uniformly ^{13}C- and ^{15}N-labeled polypeptide samples. Since ^{13}C–^{13}C homonuclear dipolar couplings can affect the observed resonances with splittings of up to 2 kHz, both heteronuclear and homonuclear ^{13}C decoupling procedures are incorporated into the pulse sequence. The experiment starts with conventional spin-lock cross-polarization from ^{1}H to ^{13}C, followed by a SEMA interval during which the ^{1}H–^{13}C dipolar couplings evolve. Continuous ^{15}N irradiation suppresses the ^{1}H–^{15}N as well as ^{13}C–^{15}N heteronuclear dipolar couplings during t_1. The ^{1}H–^{13}C heteronuclear dipolar coupling frequencies are scaled by 0.82. Immediately following t_1, the X-phase pulse θ rotates the ^{13}C magnetization by 35.5° to the magic angle, followed by flip–flop Lee–Goldburg irradiation of the ^{13}C spins and continuous irradiation of the ^{1}H and ^{15}N spins in order to suppress homonuclear ^{13}C and heteronuclear ^{1}H–^{13}C and dipolar couplings during t_2. As a result, the ^{13}C magnetization is affected only by the ^{13}C chemical shift interaction, which is scaled by a factor of 0.58, during t_2. Immediately following t_2, the X-phase ^{13}C pulse θ effects a 35.3° nutation of the ^{13}C magnetization that returns it to the transverse plane where a 90° pulse, labeled ϕ, is phase cycled to achieve quadrature detection in t_2 (*27*), with a second 90° ^{13}C pulse to flip the selected magnetization back to the transverse plane. The ^{13}C magnetization is then transferred to ^{15}N by cross-polarization (*28*). Finally, unscaled ^{15}N signals are acquired during t_3 in the presence of continuous ^{1}H and ^{13}C irradiation. Heteronuclear decoupling is accomplished throughout the experiment with continuous RF irradiation at the ^{1}H, ^{15}N, and ^{13}C resonance frequencies. The resulting spectra have intrinsically high resolution and correlate the frequencies from the $^{13}C_{\alpha}$ chemical shift, the ^{15}N chemical shift of the directly bounded amide nitrogen, and the ^{1}H–$^{13}C_{\alpha}$ dipolar coupling.

Figure 2 contains the two-dimensional ^{1}H–^{13}C dipolar coupling/^{13}C chemical shift spectrum of a single crystal sample of *N*-acetylvaline at an arbitrary orientation in the magnetic field. This spectrum was obtained with the pulse sequence diagrammed in Fig. 1A with continuous Lee–Goldburg irradiation during t_1. NAV has two inequivalent molecules in the unit cell, therefore two sets of resonances are present in the spectrum. The assignments of the individual carbon types are marked on the one-dimensional spectrum shown on the top of the two-dimensional PISEMA spectrum. For clarity, the two-dimensional PISEMA spectrum is shown slightly offset from zero frequency in the dipolar coupling frequency dimension.

The heteronuclear dipolar coupling pattern of each carbon site is clearly represented in the spectrum. Since the α-carbons and carbonyl carbons are directly bonded to ^{14}N, distinct triplets are observed in the ^{13}C chemical shift frequency dimension (*29*). In general, the ^{14}N–^{13}C triplet resonances from carbonyl carbons have very small or no ^{1}H–^{13}C dipolar splittings, while the ^{14}N–^{13}C triplets from α-carbons have relatively large ^{1}H–^{13}C dipolar couplings due to the directly bonded hydrogens. Figure 3 presents an expansion of two of the ^{13}C triplets that we observed in the spectrum of NAV in Fig. 2. On the left is one of the carbonyl carbons with almost zero ^{1}H–^{13}C dipolar coupling, and on the right is one of the α-carbons with a relatively

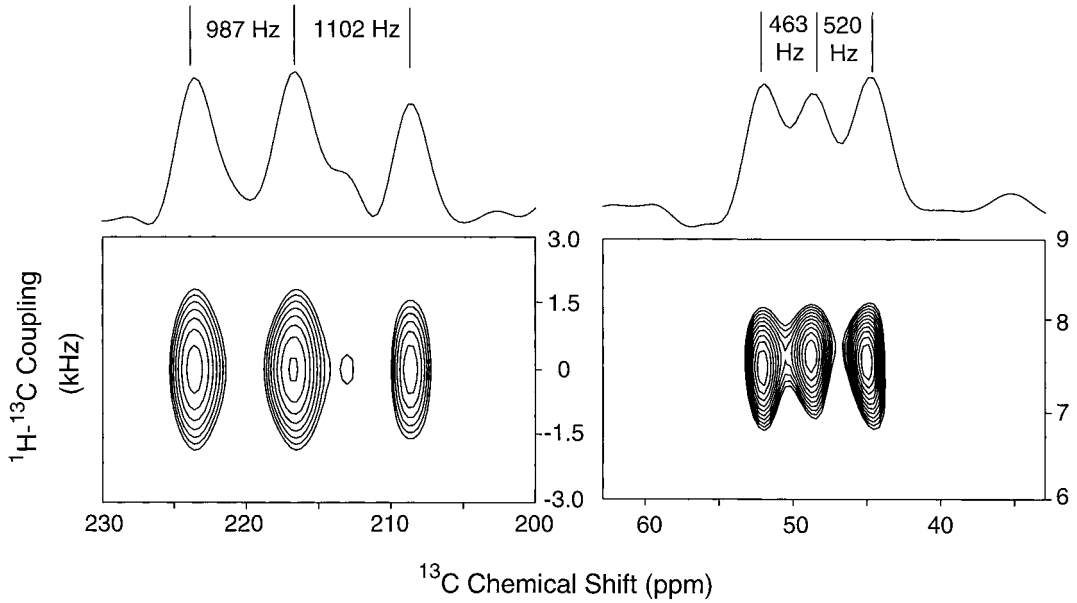

FIG. 3. Two ^{14}N–^{13}C triplets extracted from the two-dimensional spectrum in Fig. 2. The asymmetric splittings are indicated in the one-dimensional projection on the top of the spectra. Left, carbonyl carbon; right, α-carbon.

large (7.7 kHz) ^{1}H–^{13}C dipolar coupling. The splittings due to the ^{14}N–^{13}C dipolar couplings are markedly asymmetric, as shown in the one-dimensional projections on top of the spectra, because of the relatively low magnetic field and the large quadrupole couplings of ^{14}N amide sites. These asymmetric splittings provide valuable input for structure determination (*30, 31*). Neither the carboxyl carbons nor the other aliphatic carbons are directly bonded to ^{14}N, therefore single-line resonances are observed in the ^{13}C chemical shift frequency dimension from these sites.

Figure 4 contains the two-dimensional ^{1}H–^{13}C dipolar coupling/^{13}C chemical shift spectrum of a single-crystal sample of tyrosine hydrochloride at an arbitrary orientation with respect to the magnetic field. As for NAV, two sets of resonances are observed due to the two inequivalent molecules in each unit cell. Resonances from all sites on the aromatic ring of tyrosine are resolved in the two-dimensional spectrum and can be assigned based on their dipolar splitting patterns and chemical shift frequencies. At this orientation of the crystal, the observed C–H dipolar coupling frequencies differ by more than 20 kHz. This results in the highly resolved ^{1}H–^{13}C dipolar coupling frequency dimension, in spite of the use of continuous rather than flip–flop Lee–Goldburg irradiation during t_1. The assignments of each resonance to types of chemical groups are marked on the one-dimensional carbon spectrum on the top of Fig. 4.

Figure 5 shows a series of one-dimensional ^{1}H–^{13}C dipolar coupling slices extracted from the data sets used to generate the two-dimensional spectra in Figs. 2 and 4. The most likely associations between types of chemical groups and the ^{13}C chemical shift frequencies are noted. Both ^{13}COOH and ^{13}COH sites have small heteronuclear dipolar couplings and can be difficult to distinguish. In contrast, in general, ^{13}CH and ^{13}CH$_3$ groups can be readily recognized, since the ^{13}CH sites give doublets and the ^{13}CH$_3$ sites give complex patterns. In principle, all of the ^{13}CH dipolar splittings can be used to determine the angles between the C–H bonds and the direction of the applied magnetic field B_0, as well as the relative orientations between the two molecules in the unit cell.

The overall goal of this spectroscopic development is to obtain high-resolution spectra of uniformly ^{13}C- and ^{15}N-labeled proteins, since the majority of applications are to proteins prepared by expression in bacteria. The three-dimensional experiment diagrammed in Fig. 1B incorporates both homonuclear and heteronuclear decoupling schemes to give single-line resonances in all frequency dimensions. The cube in Fig. 6 is the three-dimensional ^{1}H–^{13}C dipolar coupling/^{13}C chemical shift/^{15}N chemical shift correlation spectrum obtained with the pulse sequence diagrammed in Fig. 1B. Each resonance is characterized by three frequencies and correlates the resonances from a ^{15}N amide site and its directly bonded C$_\alpha$ site for the ^{13}C- and ^{15}N-labeled sample of NAG. Resonances from carbonyl carbon sites are not shown in the spectrum because of the effects of the weak two-bond C–H dipolar couplings on the efficiency of magnetization transfer.

The experimental results presented in Figs. 2–6 demonstrate that high-resolution ^{1}H–^{13}C dipolar coupling/^{13}C chemical shift spectra can be obtained with continous or flip–flop Lee–Goldburg irradiation during SEMA intervals. It is possible to observe all of the ^{1}H–^{13}C dipolar splittings in a single spectrum, and the various types of chemical groups can be readily distinguished. The related three-dimensional, triple-resonance ex-

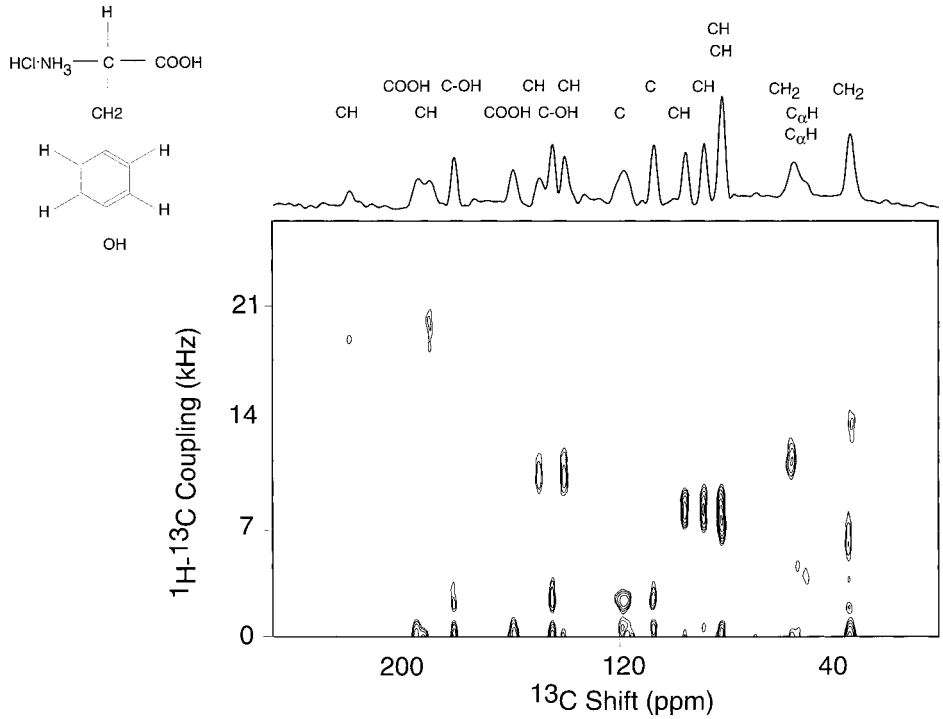

FIG. 4. Experimental two-dimensional ^{1}H–^{13}C dipolar coupling/^{13}C chemical shift spectrum of a single-crystal sample of natural abundance tyrosine hydrochloride at an arbitrary orientation with respect to the applied magnetic field. The assignments of chemical group types for each individual peak are indicated on the one-dimensional ^{13}C NMR spectrum at the top of the figure.

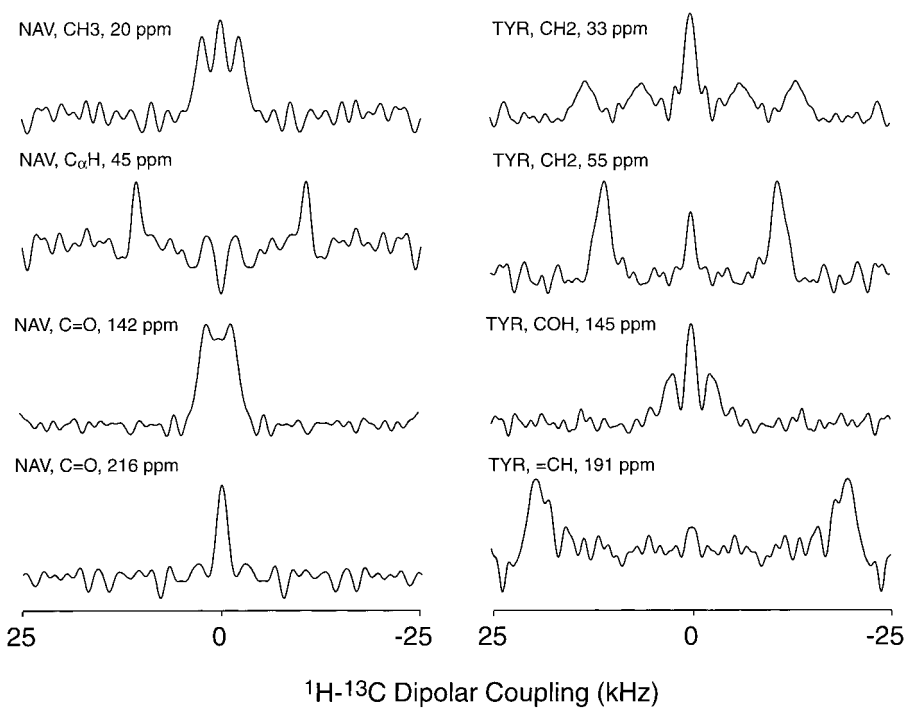

FIG. 5. A selection of one-dimensional ^{1}H–^{13}C dipolar coupling slices extracted from the two-dimensional spectra in Figs. 2 and 4. The type of the chemical group and the ^{13}C chemical shifts are indicated on with the spectral slices.

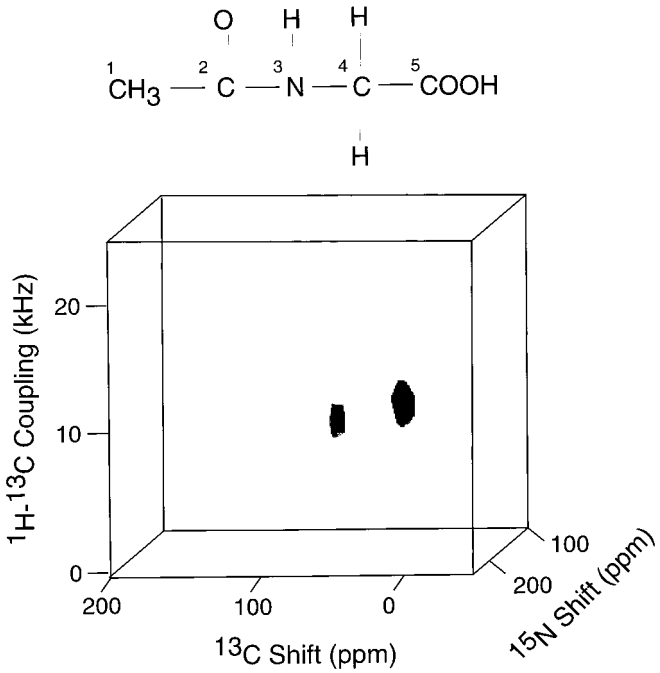

FIG. 6. Experimental three-dimensional ^{1}H–^{13}C dipolar coupling/^{13}C chemical shift/^{15}N chemical shift spectrum of a single-crystal sample of 2,4-^{13}C, 3-^{15}N NAG at an arbitrary orientation with respect to the applied magnetic field.

periment can be used to measure ^{1}H–$^{13}C_{\alpha}$ dipolar couplings in uniformly ^{13}C- and ^{15}N-labeled samples as well as other spectroscopic parameters including ^{15}N amide and $^{13}C_{\alpha}$ chemical shift frequencies. The ^{1}H–^{13}C dipolar coupling interaction provides an independent frequency dimension that can be used to resolve the overlapping ^{13}C spectral lines of oriented polypeptide samples. The inclusion of the ^{1}H–^{13}C dipolar coupling frequency also improves the precision and accuracy of backbone structures determined by solid-state NMR spectroscopy of oriented samples. Further, it provides a way of determining the orientations of all side chains, giving the potential for full three-dimensional structure determination by solid-state NMR spectroscopy of oriented samples.

EXPERIMENTAL SECTION

The solid-state NMR experiments were performed at ambient temperature on a homebuilt triple-resonance spectrometer with a 12.9-T wide-bore Magnex 550/89 magnet. The probe had a single 5-mm-ID solenoid coil triple-tuned to the ^{1}H, ^{13}C, and ^{15}N resonance frequencies of 549.8, 138.3, and 55.7 MHz, respectively. A RF field strength of 50 kHz (90° pulse width of 5 μs) was utilized on the ^{1}H, ^{13}C, and ^{15}N channels, and this corresponds to off-resonance Lee–Goldburg frequency jumps of $\pm$35.1 kHz. The two-dimensional spectra resulted from a total of 64 t_1 increments with dwell times of 20 or 40.8 μs for the continuous, Lee–Goldburg, or flip–flop Lee–Goldburg experiments, respectively. Thirty-two scans were coadded during each t_1 increment with a recycle delay of 5 s. In the three-dimensional experiment, continuous irradiation at the ^{13}C and ^{15}N resonance frequencies with RF field strengths of 40 kHz was used to provide heteronuclear decoupling. A cross-polarization mix time of 0.6 ms was used to transfer magnetization from $^{13}C_{\alpha}$ to ^{15}N amide sites. During the ^{13}C to ^{15}N cross-polarization mix time, continuous ^{1}H irradiation with a RF field strength of 83.3 kHz was applied. A total of 16 t_1 and 24 t_2 experiments were performed with dwell times of 20 and 40.8 μs, respectively. Two scans were coadded during each t_1 and t_2 increment. A recycle delay of 30 s was used in combination with a flip-back pulse to conserve ^{1}H magnetization. The experimental scaling factors of 0.81 $\pm$ 0.04 during t_1 and 0.58 $\pm$ 0.01 during t_2 are close to the theoretical values and are indicative of well-set-up experiments. The experimental NMR data were processed using Felix (Biosym Technologies). The final processed data matrix contained 64 $\times$ 128 $\times$ 128 points. The ^{13}C and ^{15}N chemical shifts are referenced with respect to the ^{13}C frequency of the deshielded peak of adamantane at 38.6 ppm and the ^{15}N frequency of liquid ammonia at 0 ppm, respectively.

The synthesis of 2,4-^{13}C, 3-^{15}N-labeled *N*-acetylglycine has been described previously (*7*). A 60-mg single crystal of 2,4-^{13}C, 3-^{15}N-labeled NAG and a 40-mg single crystal of natural abundance *N*-acetyl-D,L-valine were crystallized from aqueous solution and used in the experiment. Tyrosine hydrochloride crystals were crystallized from aqueous solution containing 10% hydrochloric acid.

ACKNOWLEDGMENTS

We thank R. McNamara for assistance with the instrumentation for the triple-resonance experiments. This research was supported by grants from the National Institute of General Medical Sciences (RO1GM29754 and R37GM24266). It utilized the Resource for Solid-State NMR of Proteins at the University of Pennsylvania, supported by Grant P41RR09731 from the Biomedical Research Technology Program, National Center for Research Resources, National Institute of Health. Z. T. Gu acknowledges support of postdoctoral fellowship 5999-99 from the Leukemia Society of America.

REFERENCES

1. C. H. Wu, A. Ramamoorthy, and S. J. Opella, High resolution heteronuclear dipolar solid state NMR, *J. Magn. Reson. B.* **109,** 270–272 (1994).
2. A. Ramamoorthy, F. M. Marassi, M. Zasloff, and S. J. Opella, Three-dimensional solid-state NMR spectroscopy of a peptide oriented in membrane bilayers, *J. Biomol. NMR* **6,** 329–334 (1995).
3. R. Jelinek, A. Ramamoorthy, and S. J. Opella, High resolution three-dimensional solid-state NMR spectra of a uniformly ^{15}N labeled protein, *J. Am. Chem. Soc.* **117,** 12348–1234 (1995).
4. F. M. Marassi, A. Ramamoorthy, and S. J. Opella, Complete resolution of the solid-state NMR spectrum of a uniformly ^{15}N-labeled membrane protein in phospholipid bilayers, *Proc. Natl. Acad. Sci. USA* **94,** 8551–8556 (1997).
5. Y. Kim, K. Valentine, S. J. Opella, S. L. Schendel, and W. A. Cramer,

Solid-state NMR studies of the membrane-bound closed state of the colicin E1 channel domain in lipid bilayers, *Protein Sci.* **7,** 342–348 (1998).

6. S. J. Opella, P. L. Stewart, and K. G. Valentine, Protein structure by solid-state NMR spectroscopy, *Q. Rev. Biophys.* **19,** 7–49 (1987).
7. Z. Gu and S. J. Opella, Three dimensional ^{13}C shift/^{1}H–^{15}N coupling/^{15}N shift solid state NMR correlation spectroscopy, *J. Magn. Reson.* **138,** 193–198 (1999).
8. W. M. Tan, Z. Gu, A. C. Zeri, and S. J. Opella, Solid-state NMR triple resonance backbone assignments in a protein, *J. Biomol. NMR* **13,** 337–342 (1999).
9. W. Veeman, Carbon-13 chemical shift anisotropy, *Prog. NMR Spectrosc.* **16,** 193–235 (1984).
10. T. M. Duncan, "A compilation of chemical shift anisotropies," Farragut Press, Madison, WI (1990).
11. C. H. Ye, R. Q. Fu, J. Z. Hu, and S. W. Ding, C-13 chemical-shift anisotropies of solid amino-acids, *Magn. Reson. Chem.* **31,** 699–704 (1993).
12. E. F. Rybaczewski, B. L. Neff, J. S. Waugh, and J. S. Sherfinski, High resolution ^{13}C NMR in solids: ^{13}C local fields of CH, CH_2, and CH_3, *J. Chem. Phys.* **67,** 1231 (1977).
13. X. Wu, S. Zhang, and X. Wu, Selective polarization inversion in solid state high resolution CP MAS NMR, *J. Magn. Reson.* **77,** 343–347 (1988).
14. A. Ramamoorthy, C. H. Wu, and S. J. Opella, Determination of ^{1}H and ^{13}C chemical shift tensors in Leu-[$^{13}C_\alpha$]Ala-Leu by three dimensional solid state NMR spectroscopy, *submitted* (1999).
15. M. T. Brenneman and T. A. Cross, A method for the analytic determination of polypeptide structure using solid state nuclear magnetic resonance: The "metric method," *J. Chem. Phys.* **92,** 1483–1494 (1990).
16. N. Tjandra and A. Bax, Large variations in $^{13}C_\alpha$ chemical shift anisotropy in proteins correlate with secondary structure, *J. Am. Chem. Soc.* **119,** 9576–9577 (1997).
17. B. Reif, M. Hennig, and C. Griesinger, Direct measurement of angles between bond vectors in high resolution NMR, *Science* **276,** 1230–1233 (1997).
18. D. W. Yang, R. Konrat, and L. E. Kay, A multidimensional NMR experiment for measurement of the protein dihedral angle ϕ based on cross-correlated relaxation between $^{1}H_\alpha$–$^{13}C_\alpha$ dipolar coupling and $^{13}C'$ (carbonyl) chemical shift anisotropy mechanisms, *J. Am. Chem. Soc.* **119,** 11938–11940 (1997).
19. P. J. Carroll, P. L. Stewart, and S. J. Opella, Structures of two model peptides: *N*-acetyl-D,L-valine and *N*-acetyl-L-valyl-L-leucine, *Acta Crystallogr. Sect. C: Cryst. Struct. Commun.* **C46,** 243–246 (1990).
20. M. N. Frey, T. F. Koetzl, M. S. Lehmann, and W. C. Hamilton, Precision neutron diffraction structure determination of protein and nucleic acid components. X. A comparison between the crystal and molecular structures of L-tyrosine and L-tyrosine hydrochloride, *J. Chem. Phys.* **58,** 2547 (1973).
21. G. B. Carpenter and J. Donohue, The crystal structure of *N*-acetylglycine, *J. Am. Chem. Soc.* **72,** 2315 (1950).
22. M. Lee and W. I. Goldburg, NMR line narrowing by a rotating RF field, *Phys. Rev. A* **140,** 1261–1271 (1965).
23. M. Mehring and J. S. Waugh, Magic angle NMR experiments in solids, *Phys. Rev. B* **5,** 3459–3471, (1972).
24. A. Bielecki, A. C. Kolbert, H. J. M. De Groot, R. G. Griffin, and M. H. Levitt, Frequency-switched Lee–Goldburg sequences in solids, *Chem. Phys. Lett.* **155,** 341–346 (1990).
25. K. Schmidt-Rohr, Complete dipolar decoupling of ^{13}C and its use in two-dimensional double quantum solid-state NMR for determining polymer conformation, *J. Magn. Reson.* **131,** 209–217 (1998).
26. A. Pines, M. G. Gibbby, and S. J. Opella, Proton-enhanced NMR of dilute spins in solids, *J. Chem. Phys.* **59,** 569–590 (1973).
27. J. Schaefer, R. A. McKay, and E. O. Stejskal, Double cross polarization NMR of solids, *J. Magn. Reson.* **34,** 443 (1979).
28. D. J. States, R. A. Haberkorn, and D. J. Ruben, A two-dimensional nuclear overhauser experiment with pure absorption phase in four quadrants, *J. Magn. Reson.* **48,** 286–292 (1982).
29. A. Naito, S. Ganapathy, K. Akasaka, and C. A. McDowell, Chemical shielding tensor and ^{13}C–^{14}N dipolar splitting in single crystals of L-alanine, *J. Chem. Phys.* **74,** 3190–3197 (1981).
30. K. V. Ramanathan and S. J. Opella, Overtone decoupling: The effects of ^{14}N overtone irradiation on ^{13}C NMR spectra of a single crystal, *J. Magn. Reson.* **78,** 367–370 (1988).
31. K. V. Ramanathan and S. J. Opella, The structures of peptides and proteins by solid-state NMR spectroscopy, *Trans. ACA* **24,** 145–153 (1988).